

HIGH-SPEED-PROPELLER WIND-TUNNEL AEROACOUSTIC RESULTS

Robert J. Jeracki and James H. Dittmar
National Aeronautics and Space Administration
Lewis Research Center

The energy saving potential of the high-speed turboprop has been discussed with increased interest in recent years (refs. 1 to 9; with many additional references in ref. 1). Gatzen's paper at this conference indicated the benefits from and the approach to applying the high-speed propeller to business-jet type of aircraft. These aircraft fly in the Mach 0.5 to 0.8 range, above the speeds of present turboprop-powered executive aircraft, and at altitudes above 9.144 km (30 000 ft) where turbojet and turbofan engines are presently used. An advanced high-speed turboprop, however, has the potential for significant fuel saving compared with these two propulsion systems. The high flight speed and altitude and other design constraints make the high-speed turboprop a unique propulsion system.

This paper will present some aerodynamic concepts, explain how these are applied to advanced propeller design, and then show results from recent wind-tunnel tests at Lewis. This should give a feeling for why the concepts were used and their importance in obtaining good aerodynamic and acoustic performance. Figure 1 shows how unique this propulsion system really would be, based on the design concepts being considered for the high-speed turboprop. Most obvious are the blade sweep, long blade chords, and, of course, the large number of blades. Other details not easily seen in this photograph will be described later. These unique features come from the need to keep a reasonable propeller size and to fly efficiently and quietly at high speed and altitude. The large fuel saving potential and the lack of an adequate data base for this new propulsion concept prompted NASA to begin a test program to verify the high-speed turboprop potential for saving energy.

AERODYNAMIC CONCEPTS

The high flight Mach number requires the designer to minimize compressibility losses. Some aerodynamic concepts that could be used are shown in figure 2. In the blade tip region compressibility loss is reduced by using thin airfoil sections and by sweeping the blade tip back, as illustrated by the two sketches at the top of the figure. In the hub region the blockage of the nacelle behind the propeller and area-ruffling, or sculpting-out of the spinner between blades, are used to reduce losses. These are illustrated by the next two sketches. Advanced airfoils designed for high performance and low noise signature were not part of these model designs, but these could be included

later as future improvements.

The effects of these concepts incorporated into a propeller design are shown in figure 3. This figure is based on the cruise condition at Mach 0.8 and presents the Mach number approaching the blade from the hub to the tip. The total Mach number, which includes both the free-stream component and the propeller rotational component, is the top curve. The Mach number starts just above the cruise Mach number at the hub, increases as the rotational velocity becomes larger, and reaches Mach 1.14 at the tip for the design conditions.

This local approach Mach number must be compared with the Mach number where each blade airfoil section enters into drag rise to evaluate how the propeller will perform. Therefore, for a thin blade with a thickness-to-blade-chord ratio of about 15 percent at the hub and down to 2 percent at the tip, isolated two-dimensional airfoil data were used to predict the Mach number at which each airfoil section would go into drag rise. That drag rise Mach number is the second curve in figure 3. Note that the local Mach number is above the drag rise Mach number from the hub to the tip and that across the entire blade is a large potential compressibility loss region. This loss region is depicted in figure 3 by the cross-hatched region.

The aerodynamic concepts shown in figure 2 were used to reduce these losses. In the tip region sweep reduces the component of velocity normal to the blade airfoil section, as is done for swept wings. So the Mach number is reduced from the local to the effective Mach number shown in figure 3. With the effective Mach number below the drag divergence Mach number in the tip region, the loss is significantly reduced. In the hub region nacelle blockage behind the propeller reduces the local Mach number through the propeller plane. That is plotted as the effective Mach number curve near the hub. Additional suppression is used here because, with the large number of blades, the hub blade sections operate as essentially a cascade or fan where blade-to-blade choking could be a problem. Area-ruling the spinner between blades gives further protection from choking by opening the flow area between the blades at the spinner. Further discussion of the application of these concepts to high-speed propeller design is given in references 1, 4, and 5, and blade structural design is covered in references 3 and 10.

PROPELLER MODEL DESIGNS

The concepts described above were used to design a series of propeller models for wind-tunnel testing in a cooperative program between Lewis and Hamilton Standard. The three basic blade planforms pictured in figure 4 represent the four propeller designs. In common are the blade tip speed of 244 m/sec (800 ft/sec), cruise power loading of 301 kW/m² (37.5 shp/ft²) (which is about four times that of a conventional propeller such as on the Electra), and eight blades. The planforms are identified by their sweeps of 0, 30°, and 45°. Here, the tip sweep is approximately the angle of the tip of the blade measured back from a radial line normal to the axis of rotation through the blade root.

The original 0 and 30° swept blades were designed using existing established analyses (ref. 11) that lacked a refined methodology to design the twist of a swept blade. Initial tests of the 30° swept design (SR-1) indicated a retwist was required (that is, redistribution of the blade load from hub to tip). The retwisted blade became the second 30° swept design (SR-1M). The 45° swept blade was swept, and the planform shaped for acoustic suppression as well as improved aerodynamic performance. More detailed discussions of the aeroacoustic design methodology are presented in references 3, 12, and 13.

Efficiency and noise level were predicted when these blades were designed. Those predicted efficiencies (listed in fig. 4) indicated improved performance with increased sweep. Those noise predictions indicated some reduction for 30° of sweep and significant reduction for the aeroacoustic 45° swept design.

The photographs in figure 5 show the 0, 30°, and 45° swept, 62.2-cm (24.5-in.) diameter propeller models installed on the Propeller Test Rig (PTR) in the Lewis 8- by 6-foot wind tunnel. The tunnel (ref. 13) has a porous wall test section to minimize any wall interactions. The PTR is powered by a 746-kW (1000-hp) air turbine using a continuous flow, 3.1×10^6 -N/m² (450-psi) air system routed through the support strut. Force and torque on the propeller are measured on a rotating balance located inside of an axisymmetric nacelle behind the propeller.

PROPELLER AERODYNAMIC PERFORMANCE

Typical test results from the 45° swept design are shown in figure 6 to give an understanding of the way data were taken and used. This is the basic propeller data plot where net thrust efficiency and a dimensionless power coefficient are plotted as ordinates. The abscissa is the advance ratio, which is proportional to the ratio of flight or advance speed to blade tip speed. As tip speed increases from windmill (no power), the advance ratio decreases as shown by the two horizontal scales. Blade angle is set and data are taken from windmill to higher power as shown by the data symbols on the power coefficient plot. The blade angle ($\beta_{3/4}$), measured at 3/4 of the propeller radius, becomes 90° when the chord of that airfoil section is aligned directly with the flight direction. As power is increased the thrust increases and, as seen in the upper data curves, the net thrust efficiency increases, reaches a peak, and then begins to drop off. Other blade angles yield similar power and efficiency curves.

At the design Mach number of 0.8, the design power loading and design tip speed give a power coefficient of 1.7 and advance ratio of 3.06. A solid line is drawn through this point on the power coefficient plot, intersecting the two lines of data shown. This solid line represents the design power at different propeller tip speeds. The efficiency at the design power can be found for each blade angle, indicated by each vertical line. Then the variation of net efficiency with advanced ratio (i.e., tip speed) at design power can be plotted as shown in figure 7. This plot is for models with area-ruled spinners at the design power loading at Mach 0.8. Curves of net efficiency versus advance ratio are compared for different sweep angles. Significant improvement can be seen in

going from 0 to 30° of sweep. The 45° swept blade shows still more improvement, especially at low advance ratios (corresponding to high tip speeds). The overall improvement at the design advance ratio of 3.06 is about 3 percent.

Other important design variations were investigated using the 30° swept designs. As noted in the description of the blade designs, there were two different twist, or loading distributions, with the same 30° swept planform. The blade design with the revised (reduced) twist was tested with both a conic and an area-ruled spinner. The performance comparison is shown in figure 8. As in the previous figure, this one presents data for the design Mach number and power loading. The original design (baseline twist) was tested with a conic spinner and is the lowest of the three data curves. Retwisting to increase the load at the tip improved the performance near the design advance ratio, where the highest efficiency for that blade-spinner combination then occurred. That reduced-twist design was also tested with an area-ruled spinner. That change improved the performance about 1 percent over the full range of tip speeds tested. This figure indicates the benefit of area-ruling and that the proper twist or loading is required to obtain high performance.

Because figures 7 and 8 summarize data at the design power, the performance at the actual design point at Mach 0.8 can be obtained as the net efficiency at the advance ratio (3.06) corresponding to the design tip speed. Similarly, net efficiency at other free-stream Mach numbers can be obtained at the same power coefficient and advance ratio as the Mach 0.8 design point. The variation of performance with free-stream Mach number is shown in figure 9 at constant power coefficient and advance ratio, for the 0, 30°, and 45° swept blade designs with area-ruled spinners. This plot is interesting because the ideal efficiency, presented as the upper dashed line, is constant across the Mach number range for a given value of power coefficient and advance ratio. The ideal efficiency is the performance of an optimum propeller with no blade drag and, so, represents only axial momentum, swirl, and tip losses. Below that line is the real world where viscous and compressibility losses occur. As the data show, those losses increase as Mach number is increased.

Again, the benefit from sweep of about 3 percent is seen at Mach 0.8. The efficiency of the 45° swept model approached the value used in the studies which showed the large fuel saving potential for the high-speed turboprop. Actually, at power loadings lower than design, the efficiency slightly exceeded the study value. However, the lower power loading would require a larger and heavier propeller for the same aircraft installation. The 45° swept blade which achieved this high performance also retains fairly high efficiency out to Mach 0.85. More performance details are given in references 1, 4, 5, and 6.

PROPELLER ACOUSTIC PERFORMANCE

Acoustic data were also taken in the tunnel, since the cabin noise at cruise conditions is of concern. The transonic propeller relative tip speed of these blade designs has the potential for generating high noise levels. This noise needs to be minimized and fuselage attenuation needs some improvement. Wall-mounted pressure transducers were used to obtain near-field acoustic data

for the propeller models. (Further details are given in refs. 15 and 16.) Wave shapes of the near-field pressure signal during blade passages are shown in figure 10. These are enhanced pressure-time traces for both the straight blade and the aeroacoustically designed 45° swept blade. The transducer closest to the propeller was used (on the tunnel wall in the plane of the propeller). As can be seen, the trace for the straight blade shows a high amplitude, steep wave shape, which approaches the classic N wave shock pattern. However, in the plot for the quieter 45° swept blade, an almost sinusoidal wave was observed which is also of considerably less amplitude. These differences in the character of the traces indicated that the aeroacoustically designed planform of the 45° swept blade has been successful in reducing the sharp pressure rise that would normally be associated with transonic helical-tip-speed propellers.

Another comparison of the benefits of sweep makes the magnitude of the noise reduction more apparent. Figure 11 is a plot of the maximum blade passage tone on the tunnel ceiling versus the helical-tip (total, including flight and rotational) Mach number. The advance ratio and power coefficient for all of the data points are approximately the design values. Variation in helical-tip Mach number is obtained by taking data at different free-stream Mach numbers. The plots for both 0 and 45° swept blades exhibit a region of sharp noise increase with increasing helical-tip Mach number, which is then followed by a region where noise levels off. The tailored sweep of the 45° design provides noise reduction over the complete range of tip speeds. Near the cruise design tip Mach number of 1.14, the reduction is about 5 to 6 dB and appears to be even larger at the lower tip speeds tested. Data in reference 16 from a 30° swept blade, together with the data shown here, indicate that increasing tip sweep delays the sharp increase in noise to a higher tip Mach number. This delay in noise rise would be expected just as sweep delays the sharp drag rise of the blades by postponing the onset of shocks in the blade tip region. The overall noise reduction at high and low tip speeds indicates the benefit of the aeroacoustic methodology of the 45° swept design.

Noise data were taken at positions in front of and behind the propeller plane on the tunnel ceiling. Figure 12 is a plot of the axial variation of the blade passage tone versus the axial position from the propeller plane plotted in propeller diameters. The ceiling itself is about 1.5 propeller diameters from the propeller tip. The same significant reduction in peak noise level for the 45° swept blade can be observed here as in figure 11. At Mach 0.8 cruise the noise from these propellers differs only slightly ahead of the propeller and tends to have the largest difference farther behind the propeller. Notice the directivity of the noise pattern. The peak noise level has dropped off significantly from the peak within a total distance of about 2 propeller diameters. This indicates that any required fuselage treatment would be limited in area. More details and data are given in references 15 and 16.

SUMMARY OF RESULTS

The noise reduction and the high measured performance show the aerodynamic and acoustic benefits of advanced propeller design concepts. High aerodynamic performance was obtained at Mach 0.8; within 1 percent of the study value used

to predict large potential fuel saving for the high-speed turboprop. Performance near 80 percent was obtained at lower-than-design power loadings. Nacelle blockage was an important part of the designs, and area-ruling was shown to be important in improving measured performance. Blade tip sweep improved aerodynamic performance about 3 percent, while the aeroacoustic design of the 45° swept propeller reduced cruise near-field noise about 6 dB.

FUTURE IMPROVEMENTS

The performance results shown are attractive, and further refinements can be made. There is now a basis for improvements in design and analysis. Figure 13 indicates the future of high-speed turboprop improvements. The lower-left circle represents the current design procedures and model results described in this paper. The propellers were eight bladed, highly loaded, and designed using established analyses, although a number of advanced concepts were incorporated. Two new further advanced models are being designed and should be tested in 1980. These models are advanced, 10-bladed designs which have greater tip sweep and lower tip speed to improve the acoustic as well as the aerodynamic performance. Some refined analyses were available for the design of these blades (ref. 12).

The results of both the present tests and those planned in 1980 will be used to achieve an initial optimum design, called SR-7. When that propeller is being designed, additional advanced analyses (described in Bober's paper at this conference and ref. 11) will be available to further enhance the design process. Testing that design will conclude the present wind tunnel program on propeller performance and noise. Another approach which is under study by NASA as a future research area to further improve performance is to recover the thrust lost in the swirl of the propeller slipstream. The swirl loss for these highly loaded propellers can be as much as 6 to 8 percent in efficiency. Methods being considered for swirl recovery are coaxial counterrotation, wing contouring behind the propeller (to act like a stator), and the introduction of stators behind the propeller. This continued effort, shown in figure 13, is expected to allow future propellers to be designed for high-speed flight with both higher efficiency and significantly lower cruise noise.

REFERENCES

1. Jeracki, Robert J.; Mikkelson, Daniel C.; and Blaha, Bernard J.: Wind Tunnel Performance of Four Energy Efficient Propellers Designed for Mach 0.8 Cruise. NASA TM-79124, 1979 or SAE Paper 790573, Apr. 1979.
2. Nored, Donald L.: Fuel Conservative Aircraft Engine Technology. NASA TM-78962, 1978.
3. Dugan, James F. Jr.; Gatzen, Bernard S.; and Adamson, William M.: Prop-Fan Propulsion - Its Status and Potential. SAE Paper 780995, Nov. 1978.

4. Mikkelson, Daniel C.; et al.: Design and Performance of Energy Efficient Propellers for Mach 0.8 Cruise. NASA TM X-73612, 1977 or SAE Paper 770458, Mar. 1977.
5. Black, D. M.; Menthe, R. W.; and Wainauski, H. S.: Aerodynamic Design and Performance Testing of an Advanced 30° Swept, Eight Bladed Propeller at Mach Numbers from 0.2 to 0.85. NASA CR-3047, 1978.
6. Rohrbach, Carl: Prop Fan Offers Low Fuel Consumption at Today's Flight Speeds and Altitudes. AIAA Paper 76-667, July 1976.
7. Jackson, A. H., Jr.; and Gatzen, B. S.: Multi-Mission Uses for Prop-Fan Propulsion. Variable Geometry and Multicycle Engines, AGARD-CP-205, Advisory Group For Aerospace Research and Development, Paris, 1977, pp. 15-1 to 15-13.
8. Kraft, G. A.; and Strack, W. C.: Preliminary Study of Advanced Turboprops for Low Energy Consumption. NASA TM X-71740, 1975.
9. Rohrbach, C.; and Seery, M. E.: A New Look at the Turboprop. AIAA Paper 75-1208, Sept. 1975.
10. Cornell, R. W.; and Rothman, E. A.: Design and Analysis of Prop-Fan Blades. AIAA Paper 79-1116, June 1979.
11. Bober, L. A.; and Mitchell, G. A.: Summary of Advanced Methods for Predicting High Speed Propeller Performance. NASA TM-81409, 1980, or AIAA Paper 80-0225, Jan. 1980.
12. Metzger, F. B. Rohrbach, C.: Aeroacoustic Design of the Prop-Fan. AIAA Paper 79-0610, Mar. 1979.
13. Hanson, D. B.: Near Field Noise of Supersonic Propellers in Forward Flight. AIAA Paper 76-565, July 1976.
14. Swallow, Robert J.; and Aiello, Robert A.: NASA Lewis 8- by 6-Foot Supersonic Wind Tunnel. NASA TM X-71542, 1974.
15. Dittmar, James H.; Blaha, Bernard J.; and Jeracki, Robert J.: Tone Noise of Three Supersonic Helical Tip Speed Propellers in a Wind Tunnel at 0.8 Mach Number. NASA TM-79046, 1978.
16. Dittmar, James H.; Jeracki, Robert J.; and Blaha, Bernard J.: Tone Noise of Three Supersonic Helical Tip Speed Propellers in a Wind Tunnel. NASA TM-79167, 1979.

ADVANCED LOW ENERGY TURBOPROP MODEL
MACH 0.8 CRUISE

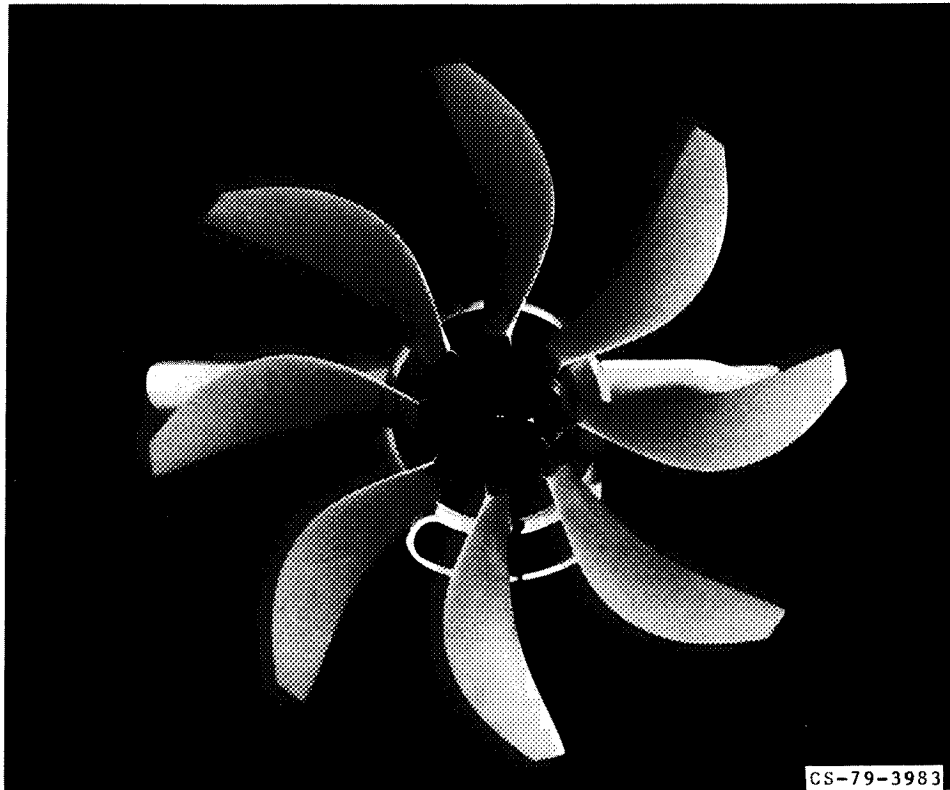


Figure 1

ADVANCED AERODYNAMIC CONCEPTS

REDUCED THICKNESS



BLADE SWEEP



NACELLE BLOCKAGE



SPINNER AREA RULING



ADVANCED AIRFOILS

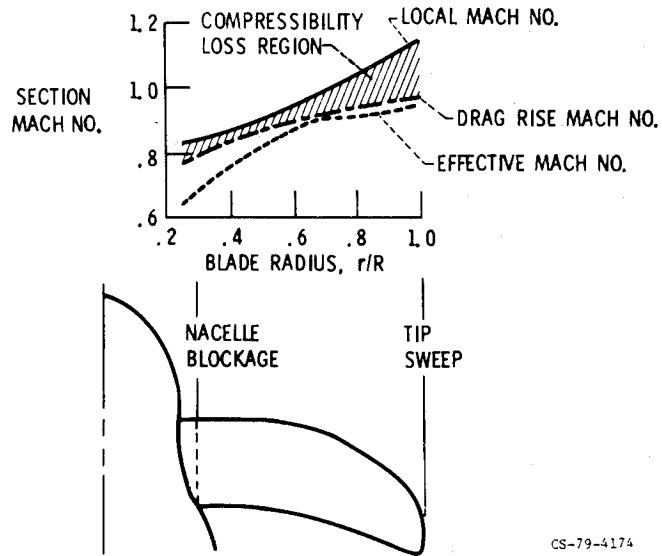


CS-79-1472

Figure 2

EFFECTS OF ADVANCED AERODYNAMIC CONCEPTS

$M_0 = 0.8$

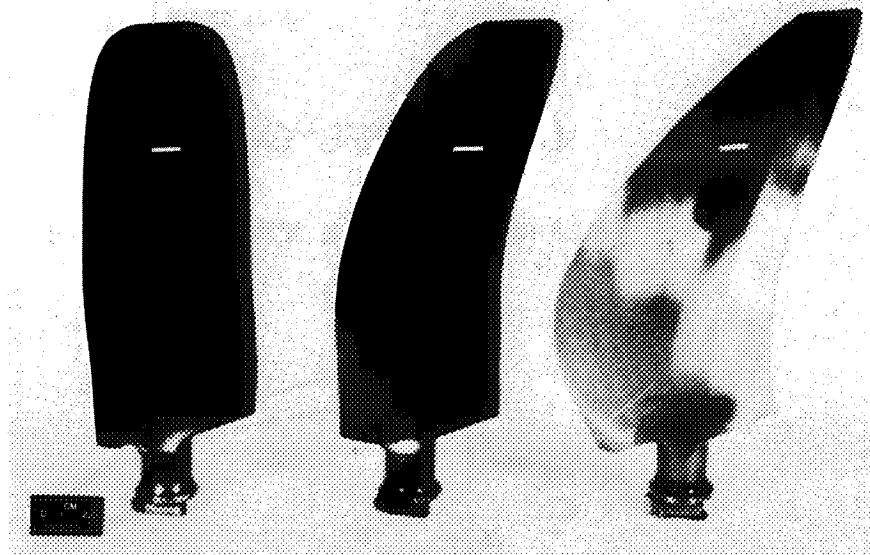


CS-79-4174

Figure 3

PROPELLER MODEL COMPARISON

TIP SPEED, ft/sec 800
 POWER LOADING, hp/ft² 37.5
 NO. OF BLADES 8



	SR-2	SR-1, 1M	SR-3
TIP SWEEP ANGLE, deg	0	30	45
PREDICTED DESIGN EFF, %	76.6	78.9, 79.3	81.1
PREDICTED DESIGN NOISE REDUCTION, ΔdB	REF.	-2	-6

CS-79-4176

Figure 4

INSTALLATION OF PROPELLER MODELS IN THE 8X6 WIND TUNNEL

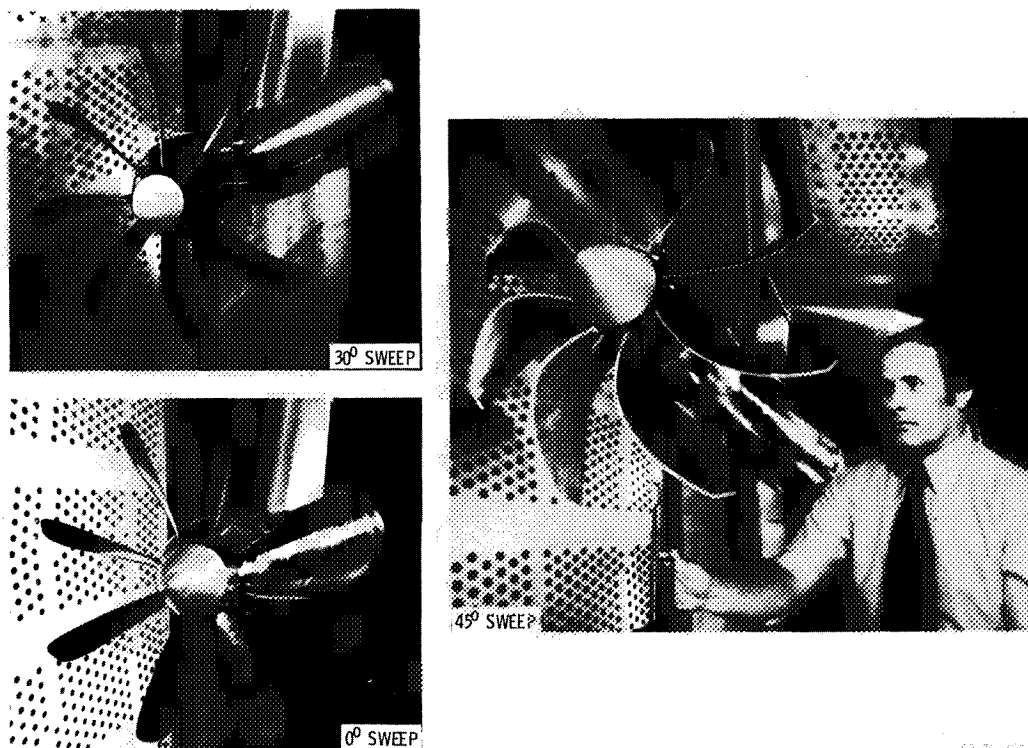
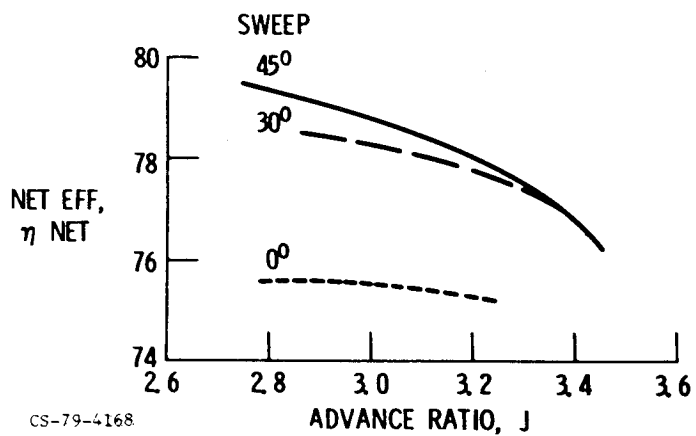


Figure 5

EFFECT OF SWEEP ON NET EFFICIENCY

AREA RULED; MACH 0.8; 100% DESIGN POWER LOADING



CS-79-4168

Figure 6

BASIC MEASURED PERFORMANCE

45° SWEEP; $M_0 = 0.8$

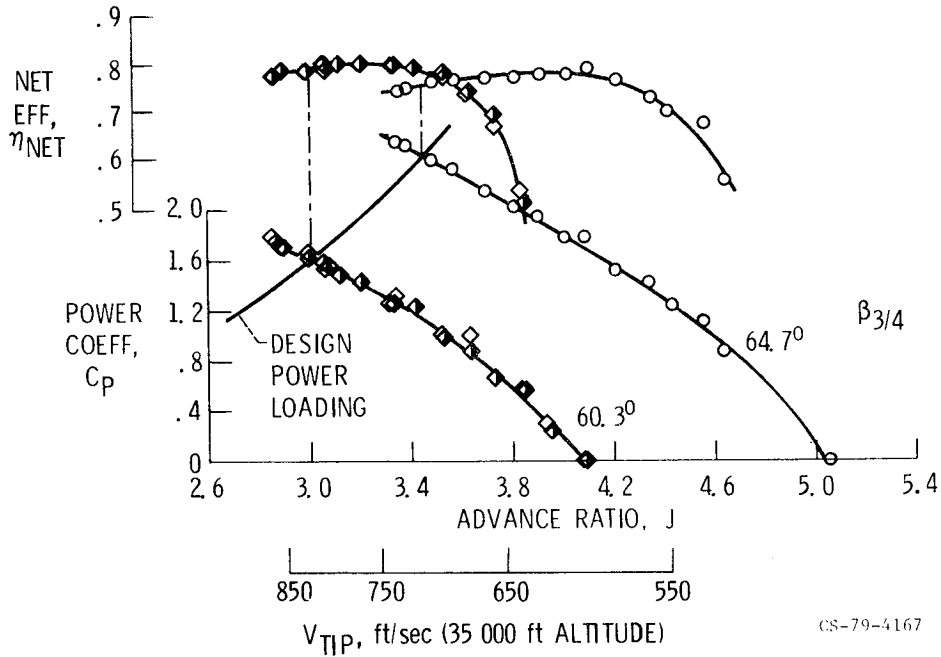


Figure 7

EFFECT OF TWIST AND AREA RULING ON NET EFFICIENCY

30° SWEEP; MACH 0.8; 100% DESIGN POWER

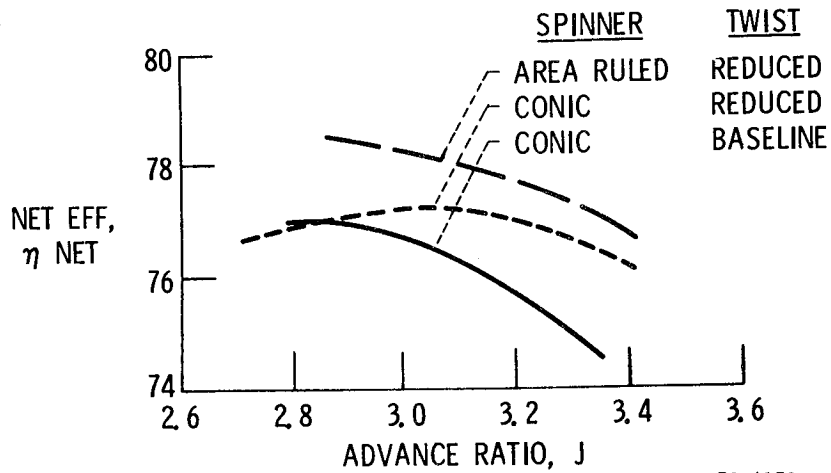


Figure 8

HIGH SPEED PROPELLER PERFORMANCE SUMMARY

AREA RULED SPINNER

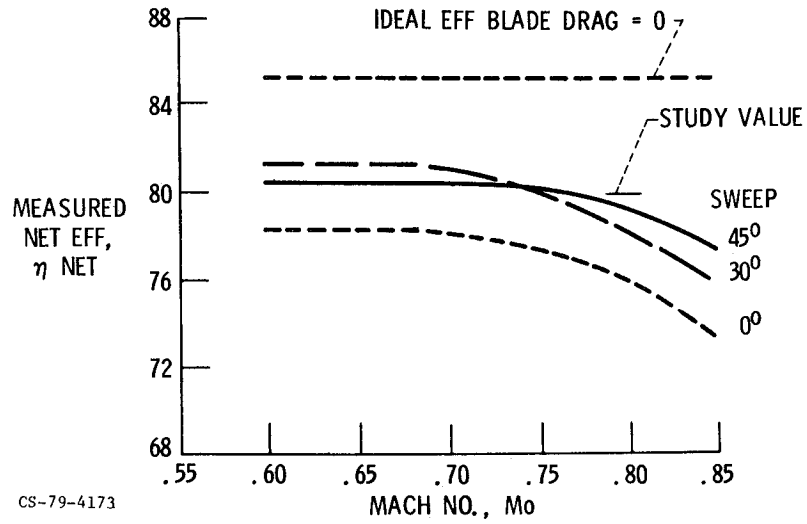


Figure 9

EFFECT OF SWEEP ON ACOUSTIC PRESSURE SIGNAL

$M_o = 0.8$; NEAR DESIGN CONDITIONS; NEAR FIELD

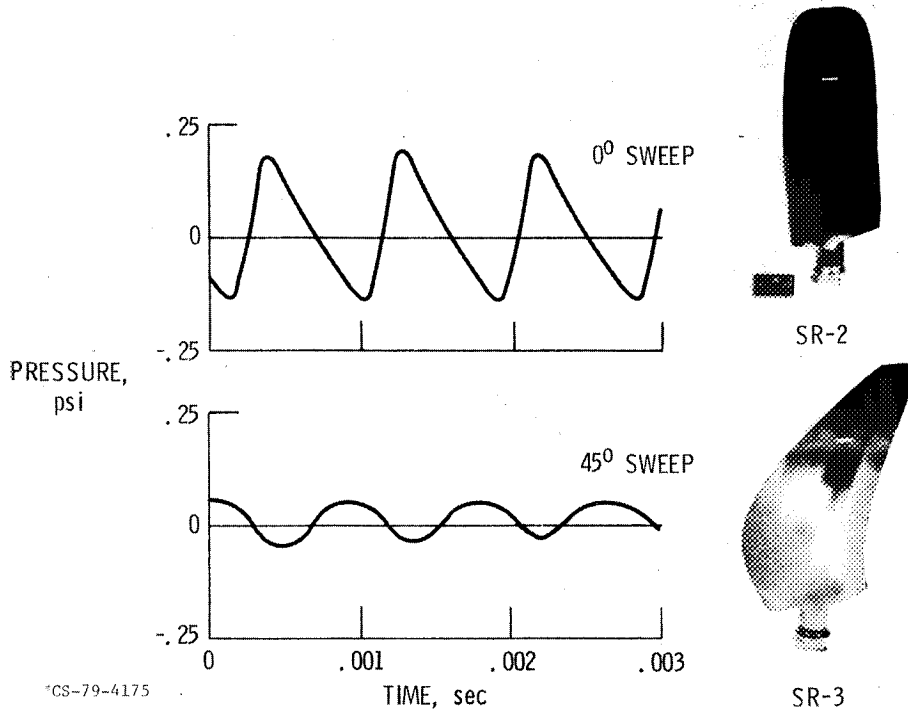


Figure 10

EFFECT OF TIP MACH NUMBER ON MEASURED NOISE

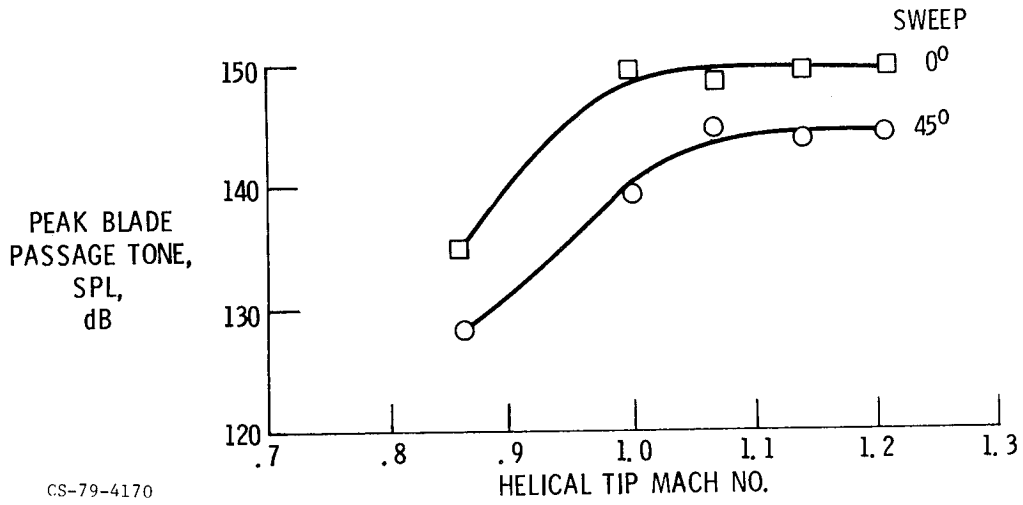


Figure 11

DIRECTIVITY OF MEASURED NOISE

$M_0 = 0.8$; NEAR DESIGN CONDITIONS; NEAR FIELD

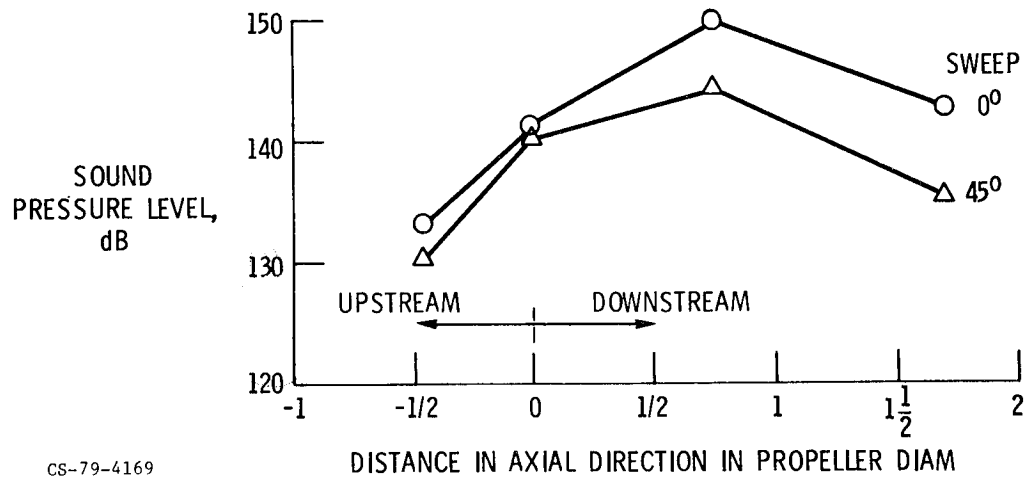
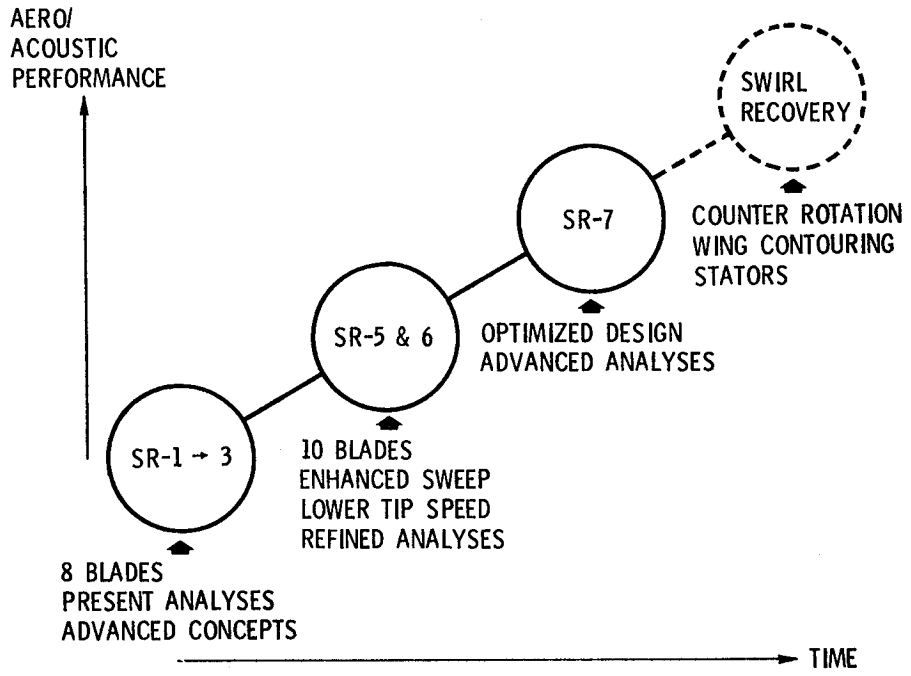


Figure 12

HIGH SPEED PROPELLER RESEARCH PROGRAM



CS-79-4171

Figure 13